Observing Manual for DDRAGO

Alan M. Watson alan@astro.unam.mx

Instituto de Astronomía Universidad Nacional Autónoma de México

12 September 2025

Contents

1	Inti	roduction	3				
2	Overview						
3	Cur	rent State	5				
4	Pha	ase 1	8				
	4.1	Mexican Phase 1	8				
	4.2	French Phase 1	8				
	4.3	Sensitivity	8				
	4.4	Overheads	9				
	4.5	Calibration	9				
5	Pha	ase 2	10				
6	Pha	ase 3	12				
	6.1	Progress	12				
	6.2	Data Files	12				
	6.3	FITS Header Records	13				
	6.4	Downloading Data	14				
	6.5	Acknowledgements in Publications	16				
7	Filt	ers and System Efficiency	17				
	7.1	Filters	17				
	7.2	Transformations	18				
	7.3	System Efficiency	18				
	74	Zero-Points	19				

8	Det	ectors	27
	8.1	Detectors and Channels	27
	8.2	Read Modes	28
	8.3	Format	28
	8.4	Bias and Dark Correction	30
		8.4.1 Bias Pedestal Removal	30
		8.4.2 Residual Bias and Dark Correction	31
	8.5	Orientation on Sky	31

Introduction

This observing manual describes the DDRAGO instrument on the COLIBRÍ telescope. It is organized as follows:

- Chapter 2 contains a one-page overview of the instrument to help you to quickly decide if DDRAGO is relevant for your science.
- Chapter 3 contains summarizes the current state of the instrument, in particular imperfections.
- Chapter 4 describes phase 1 of the observation process: requesting time.
- Chapter 5 describes phase 2 of the observation process: planning observing blocks.
- Chapter 6 describes phase 3 of the observation process: receiving data.
- The remaining chapters give a technical description of the instrument intended for observers.

The latest release of this manual is available in PDF at:

https://github.com/unam-transients/ddrago-observing-manual/blob/main/PDF.md

The members of the science operations team for COLIBRÍ are:

• Alan M. Watson <alan@astro.unam.mx>

They are available to help you with any aspect of observing with DDRAGO and COLIBRÍ.

Overview

This chapter aims to provide a one-page overview of DDRAGO to allow you to understand whether it is relevant for your science.

- DDRAGO is a two-channel optical imager for the 1.3-meter COLIBRÍ telescope at the Observatorio Astronómico Nacional.
- Each channel has a $4k \times 4k$ CCD. The pixel scale is 0.38 arcsec/pixel and the field size is 25.9 arcmin.
- The blue channel has filters that are very close to Pan-STARRS g, r, and i, a wide filter gri that passes from the blue edge of g to the red edge of i, and a B filter.
- The red channel has filters that are very close to Pan-STARRS *z* and *y* and a wide filter *zy* that passes from the blue edge of *z* and thus is similar to SDSS *z*.
- The 10σ sensitivity is typically AB ≈ 20 in 60 seconds in bright time.
- The read time is 2.4 to 7.0 seconds, depending on binning and window.
- The telescope is located at 115.4646 deg east and 31.0449 deg north, and at an altitude of 2792 meters.
- The telescope has an altitude-azimuth mount and can point anywhere above a zenith distance limit of 73.4 deg, which corresponds to an airmass of 3.5. However, the telescope cannot currently track well within 10 deg of the zenith.

Current State

The instrument was installed in November and December 2024, and we are still working to optimize its performance. The current state of the instrument and its associated systems is as follows:

- The blue channel is operational and works as expected.
- The red channel is operation and works largely as expected. However:
 - Compared to the blue CCD, the red CCD shows worse artifacts above and below bright sources, and we anticipate working with the vendor to tune the CCD voltages and improve this.
 - There is vignetting in the corners of the red CCD as the filter wheel has an incorrect rotation. We hope to correct this in November 2025.

Both of these problems can be seen in Figure 3.1.

- The telescope is operational and working largely as expected. However:
 - We have not completed optical alignment of the telescope. As a result of this, we see field-depended comma in both detectors. Nevertheless, the instrument has given images with FWHM of 0.8 arcsec in the center of the field, but the FWHM is worse away from the field center. We hope to complete alignment in November 2025.
 - The telescope tracking is not as good as we anticipated; although short exposures often have a FWHM of less than 1.0 arcsec, exposures of sixty seconds typically have a FWHM of about 1.2 arcsec. We will work in September 2025 to improve the pointing map and hence the tracking.

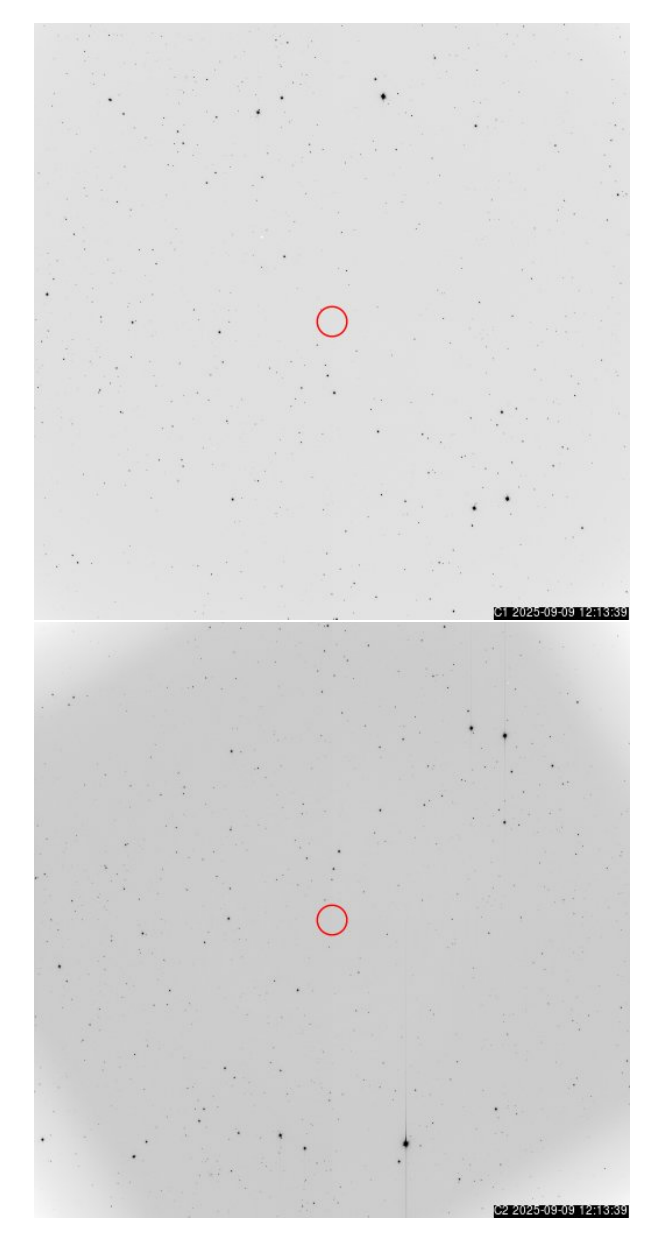


Figure 3.1: Typical images in the blue channel (above) and red channel (below). Note that the red channel is flipped vertically with respect to the blue channel because of the reflection off the second dichroic. Note also the vignetting in the red channel caused by the incorrect orientation of the filters and the trails above and below bright stars.

- The automatic data-processing pipeline is not yet available. We still do not have a date for when it will be available.
 - However, we have an engineering pipeline that is capable of stacking images and doing a simple sky subtraction. It requires some manual tuning (selecting a star for alignment and determining the fraction of frames to reject). It does not perform astrometric or photometric calibration or produce source catalogs. If you are interested in this pipeline, please contact Alan Watson <a href="mailto:slange-align: linear linea
- The scheduler is not yet fully integrated. Observations have to be programmed by hand, which limits flexibility and favors blocks that are simpler to program.

Phase 1

This chapter contains information likely to be useful in phase 2 of the observing process: requesting observing time. If you have doubts or special requirements, we recommend that you contact the science operations team.

4.1 Mexican Phase 1

The Mexican astronomical community receives 32.5% of the time on COL-IBRÍ. The process for applying for this time is managed by the Jefatura de Astronomía Observacional of the Instituto de Astronomía and the Comisión de Asignación de Tiempo de Telescopio. For more information, see:

https://jao.astroscu.unam.mx/

4.2 French Phase 1

The French astronomical community receives 22.5% of the time on COLIBRÍ. The process for applying for this time is to be determined.

4.3 Sensitivity

A simple exposure-time estimator is available here:

https://github.com/unam-transients/ddrago-observing-manual/blob/main/ETE.md

The estimator is a spreadsheet in Google Sheets. To use it:

- 1. Make your own copy by selecting File \rightarrow Make a Copy in the menus.
- 2. In your copy, change the values of the SNR, AB magnitude, and image FWHM to correspond to your science case and expected conditions.
- 3. Note the estimated exposure times in dark and bright conditions.

We do not recommend single exposures of longer than 60 seconds. For more sensitivity, we recommend taking multiple exposures of 60 seconds or less. We offer random dithering in a circle and dithering on a grid with up to 9 points per grid. The default size of the dither pattern is 1 arcmin diameter or 1 arcmin square, but this can be adjusted for each observation.

4.4 Overheads

To account for overheads, conservatively, you should allow:

- 10 seconds for readout
- 5 seconds for changing filters
- 10 seconds for dithering
- 30 seconds for the initial pointing

4.5 Calibration

We routinely take flat field, bias, and dark images. We do not routinely observe photometric standards; we typically calibrate our images from the Pan-STARRS or SkyMapper catalogs.

Phase 2

This chapter contains information likely to be useful in phase 2 of the observing process: planning observing blocks.

Each program will designate a single technical contact person. All communication with the science operations team will be through this contact person.

Approved observing programs are split into *observing blocks*. We aim to keep individual observing blocks to no more than about 30 minutes of real time (i.e., 24×60 -second exposures plus overheads). If more data are required, we recommend repeating blocks.

For each observing block, the science operations team will require the following information:

- Target name. This is strictly optional, but we find it useful.
- Program number. This will be assigned to each approved program by the science operations team.
- Target number. We recommend using a distinct target number for each target.
- Pointing J2000 coordinates.
- Filters.
- Number of exposures in each filter.
- Exposure time per exposure (default is 60 seconds).
- If you want to use random dithers, the dither circle diameter (default is 1 arcmin). If you want to dither on a grid, the number of grid points (up to 9) and the size of the grid.

- Constraints on airmass (by default below airmass 2), hour angle, and date.
- Whether the block should be run once, multiple times, or repeatedly (i.e., every second night).

Once the science operations team has this information, they will program and execute your blocks.

Phase 3

This chapter contains information likely to be useful in phase 3 of the observing process: receiving data.

6.1 Progress

The science operations team will inform the technical contact person when their blocks have run.

6.2 Data Files

The data files are created subdirectories whose names are the program, block, and visit identifiers. For example, the files for program 2022A-2001, block 10, visit 0 are created in the directory

2022A-2001/10/0/

The base name of each image created by the executor is the UTC time in ISO 8601 basic combined format followed by the channel name (e.g., CO, C1, C2, ...), followed by a letter indicating the type of exposure (o for object, f for flat, b for bias, and d for dark).

In COLIBRÍ, CO refers to the OGSE test camera, C1 to the blue channel of DDRAGO, and C2 to the red channel of DDRAGO.

For example,

20220405T072311C1o 20220405T072341C1b

20220405T072351C1f 20220405T072411C1d

For each image there are two files: the full FITS image compressed losslessly with fpack (with suffix .fz) and a text version of the header (with suffix .fits.txt). In the text version, each record is separated with a newline character.

FITS images compressed with fpack can be read by AstroPy (although you need to select hdu[1] rather than hdu[0]) and SAOImage DS9.

6.3 FITS Header Records

The FITS header records are largely self-documented by comments. However, these are the most relevant header records for searching for particular data:

- DATE-OBS: The UTC date of the start of the exposure.
- INSTRUME: The channel (e.g., CO, C1, C2, ...).
- EXPTIME: The exposure time (seconds).
- EXPTYPE: The exposure type (e.g., object, flat, bias, dark).
- FILTER: The selected filter name.
- DTDS: The detector, SI 1110-167 for the blue CCD and SI 1110-185 for the red CCD.
- BINNING: The detector binning (pixels).
- PRPID: The proposal identifier (integer).
- BLKID: The block identifier (integer).
- VSTID: The visit identifier (integer).
- STRSTRA: The J2000 RA of the target at the start of the exposure (degrees).
- STRSTDE: The J2000 declination of the target at the start of the exposure (degrees).
- STROBHA: The observed HA of the target at the start of the exposure (degrees).
- STROBDE: The observed declination of the target at the start of the exposure (degrees).

- STROBAZ: The observed azimuth of the target at the start of the exposure (degrees).
- STROBZ: The observed zenith distance of the target at the start of the exposure (degrees).
- STROBAM: The observed airmass of the target at the start of the exposure
- SMNZD: The observed zenith distance of the Moon at the start of the exposure (degrees).
- SMNIL: The illuminated fraction of the Moon at the start of the exposure.
- SMNTD: The distance between the target and the Moon at the start of the exposure (degrees).
- SSNZD: The observed zenith distance of the Sun at the start of the exposure (degrees).

For each record that begins with S and refers to the start of the exposure, there is a corresponding record that begins with E and refers to the end of the exposure. So, for example, STROBAM gives the airmass at the start of the exposure and ETROBAM gives the airmass at the end of the exposure.

6.4 Downloading Data

Data are available from transients.astrosen.unam.mx, a server in Ensenada. We shortly hope to have a second server in Mexico City. The technical contact of each program will be provided with an account name and password for the server.

Data are distributed using rsync. We recommend reading the man page or a tutorial for rsync. Each program is assigned its own "module" in the terminology of rsync.

We have noted deficiencies in the rsync command in macOS. We recommend either downloading data from a Linux machine or installing the Homebrew version of rsync (with the command brew install rsync, assuming Homebrew is already installed) and then using /opt/homebrew/bin/rsync instead of plain rsync.

On the rsync server, files are organized in directories as follows:

<date>//clate>//<block-identifier>/<visit-identifier>/

The date is in the form YYYYMMDD. The program identifiers have the form <semester>-<number>. For early science observations, the block and visit identifiers are determined by the science operations team who typically assign a different block identifier to each target and use visit identified 0 for all science exposures.

We provided to each program raw flats, biases, and darks in addition to their science data. The flats are in program <semester>-0001, biases in <semester>-0002, and darks in <semester>-0003.

Here are some examples of useful commands. We assume the program identifier is 2025A-2081 and the passwords is PASSWORD.

1. List all files at the top level in the archive:

```
RSYNC_PASSWORD=PASSWORD \
rsync -a rsync://2025A-2081@ratir.astrosen.unam.mx/2025A-2081/
```

2. List all files at the second level in the archive:

```
RSYNC_PASSWORD=PASSWORD \
rsync -a rsync://2025A-2081@ratir.astrosen.unam.mx/2025A-2081/*/
```

3. List all files in the archive:

```
RSYNC_PASSWORD=PASSWORD \
rsync -a rsync://2025A-2081@ratir.astrosen.unam.mx/2025A-2081/
```

4. Copy all files in the archive into the current directory, maintaining the directory structure:

```
RSYNC_PASSWORD=PASSWORD \
rsync -a rsync://2025A-2081@ratir.astrosen.unam.mx/2025A-2081/ .
```

5. Copy all science files in the archive into the current directory, maintaining the directory structure:

```
RSYNC_PASSWORD=PASSWORD \
rsync -a rsync://2025A-2081@ratir.astrosen.unam.mx/2025A-2081/2025A-2081/ .
```

6. Copy the science files from 2025-02-28 into the current directory, maintaining the directory structure:

```
RSYNC_PASSWORD=PASSWORD \
rsync -a rsync://2025A-2081@ratir.astrosen.unam.mx/2025A-2081/2025A-2081/20250228/ .
```

7. Copy the flat field files from 2025-02-28 into the current directory, maintaining the directory structure:

```
RSYNC_PASSWORD=PASSWORD \
rsync -a rsync://2025A-2081@ratir.astrosen.unam.mx/2025A-2081/2025A-0001/20250228/ .
```

6.5 Acknowledgements in Publications

In publications that make use of data acquired with DDRAGO, we request that you cite these papers on the telescope and instrument at an appropriate point:

- Basa et al. (2022)
- Langarica et al. (2024)

We also request that you include this text in the acknowledgments:

The data [or some of the data] used in this paper were acquired with the DDRAGO instrument on the COLIBRÍ telescope at the Observatorio Astronómico Nacional on the Sierra de San Pedro Mártir. COLIBRÍ and DDRAGO are funded by the Universidad Nacional Autónoma de México (CIC and DGAPA/PAPIIT IN109418 and IN109224), and CONAHCyT (1046632 and 277901). COL-IBRI received financial support from the French government under the France 2030 investment plan, as part of the Initiative d'Excellence d'Aix-Marseille Université-A*MIDEX (ANR-11-LABX-0060 - OCEVU and AMX-19-IET-008 - IPhU), from LabEx FO-CUS (ANR-11-LABX-0013), from the CSAA-INSU-CNRS support program, and from the International Research Program ERI-DANUS from CNRS. COLIBRÍ and DDRAGO are operated and maintained by the Observatorio Astronómico Nacional and the Instituto de Astronomía of the Universidad Nacional Autónoma de México.

There is no requirement to include members of the science operations team as authors on any publication that results from these observations in early science time or time awarded by the TACs. However, if you consider that the engineering or science operations teams have been especially helpful, you might consider mentioning them in the acknowledgments.

Filters and System Efficiency

7.1 Filters

The DDRAGO filters are summarized in Table 7.1.

The blue channel has g, r, and i filters that are very similar to the corresponding Pan-STARRS filters, a wide gri filter that passes from the blue edge of g to the red edge of i and is very similar to the Pan-STARRS i0 filter, and a i2 filter. (It can be somewhat confusing that the blue channel has red i3 and infrared i4 filters, but it's too late to change this established usage.)

The red channel has z and y filters that are very similar to the corresponding Pan-STARRS filters and a wide zy filter that passes from the blue edge of z and thus is similar to SDSS z.

The g, r, i, z, y, gri, and zy filters are interference filters on fused silica substrates. The B filter is a conventional cemented assembly of colored glasses.

The DDRAGO i and z filters were deliberately designed to be slightly different from their Pan-STARRS equivalents (Tonry et al. 2012). The Pan-STARRS i and z filters overlap slightly and cross at about 818 nm. The DDRAGO i and z filters are separated, with the i filter having its half-maximum at 812 nm and the r filter at 825 nm. This is so that the band-passes are largely defined by the filters and not by the D2 transition from reflectance to transmittance, which depends on polarization. This is especially important in DDRAGO, since there are reflections from inclined surfaces at M3, D1, and D2, and these rotate as the telescope tracks a field. The same considerations apply to the gri and zy filters. These separations can most clearly be seen in Figures 7.2 and 7.3.

Table 7.1: Filters

Filter	$\lambda_{ m S}$	$\lambda_{ m L}$	Δλ nm	$ar{\eta}$	n_0 e/s	Color Term
	11111	11111			<u> </u>	
	Blue Channel					
B	386.6	486.3	101.4	0.32	2.5×10^{9}	$+0.24\times(B-V)$
g	397.0	549.1	152.2	0.40	5.3×10^9	$-0.05\times(g-r)$
r	553.5	694.7	141.3	0.40	5.0×10^9	$+0.00 \times (g-r)$
i	690.4	812.1	121.7	0.39	3.4×10^{9}	$-0.04 \times (g-r)$
gri	399.1	811.6	412.8	0.39	1.3×10^{10}	$-0.07\times(g-r)$
	Red Channel					
z	825.9	915.1	89.6	0.33	1.5×10^9	$+0.01 \times (r-i)$
у	917.8	972.8	57.4	0.26	7.4×10^{8}	
zy	826.7	939.7	125.2	0.35	2.2×10^{9}	$+0.09\times(r-i)$

7.2 Transformations

Table 7.1 shows typical color terms for the transformations from natural magnitudes to the corresponding magnitudes in the Pan-STARRS and Landolt systems. We transform gri to Pan-STARRS r, not to Pan-STARRS w, and z and zy to SDSS z, not to Pan-STARRS z. The color terms are in the sense

Standard magnitude =
$$DDRAGO$$
 magnitude + color term. (7.1)

For most filters, the color terms are small. The exception is B, for which the color term is +0.24(B-V), and zy, for which the color term against z is +0.09(r-i). This is not unexpected; matching B is notoriously difficult with CCDs and our zy is expected to be redder than just z.

7.3 System Efficiency

We have modeled the system efficiency of the instrument at 1.5 airmasses, taking into account:

- The continuum absorption 300 nm to 2000 nm calculated using the "k-model" from Schuster & Parrao (2001), without ozone, and extrapolated from the last data point using their assumed RC index of -4.05 and derived aerosol index of -0.87.
- The atmospheric line-absorption spectrum above 850 nm generated using ATRAN (Lord 1992), made available on the SOFIA web site by Dr. William Vacca. The altitude was specified as 2790 meters and, following advice on the web page, the latitude was left at the default

of 39 degrees. We assume an airmass of 1.5 and a water vapor burden of 2.8 mm (the median value given by Otárola, Hiriart, & Pérez-León (2009). The lower wavelength limit of 0.85 µm is a limitation of ATRAN. It means that the absorption-line spectrum does not contain absorption from either the strong A-band (760 to 763 nm) and B-band (686 to 689 nm) or from other weaker lines.

- Three reflections from aluminium. We use the measurement reported by Boccas et al. (2006) for a *fresh* aluminum coating at Gemini. As the mirrors age, the reflectivity will decrease.
- Models of the transmissions of L1, L2, L3, and L4, including antireflection coatings and internal absorption.
- Vendor-supplied transmission and reflectance measurements for D1, D2, and the filters.
- Vendor-supplied transmission date for the CCD windows and quantum efficiency data for the CCDs.

Figure 7.1 shows the major components of the total system efficiency without filters — the atmosphere, the telescope, and the efficiencies of the blue and red channels including both optics and the detector — and the total system efficiencies in the blue and red channels.

Figures 7.2 and 7.3 show the transmission of the filters alone and the system efficiency including the filters. They show how the dichroic transition in D2 modifies slightly the red edges of the i and gri filters and the blue edges of the z and zy filters and how the detector fall-off modifiers significantly the response in the z, y, and zy filters.

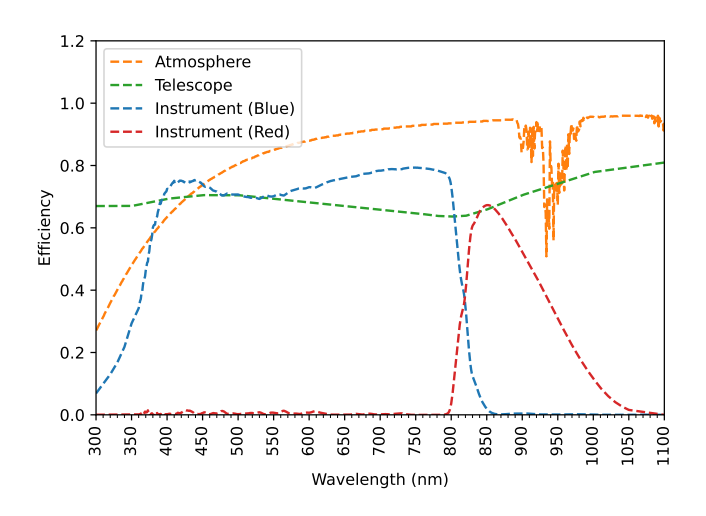
Figures 7.4 and 7.7 show in detail the total system efficiency η for each filter. Table 7.1 gives the full-width-at-half-maximum $\Delta\lambda$ and the short and long half-maximum wavelengths λ_S and λ_L for the total system efficiency. It also gives the mean efficiency $\bar{\eta}$, defined by

$$\bar{\eta}\Delta\lambda \equiv \int \eta \, d\lambda. \tag{7.2}$$

The mean efficiency would be the efficiency of a rectangular filter with width $\Delta \lambda$ and with the same integrated efficiency $\int \eta \, d\lambda$ as the real filter.

7.4 Zero-Points

Table 7.1 also gives the measured zero points n_0 for each filter. In practical terms, the zero point n_0 is the expected signal in e/s from a source with zero AB magnitude at all wavelengths.



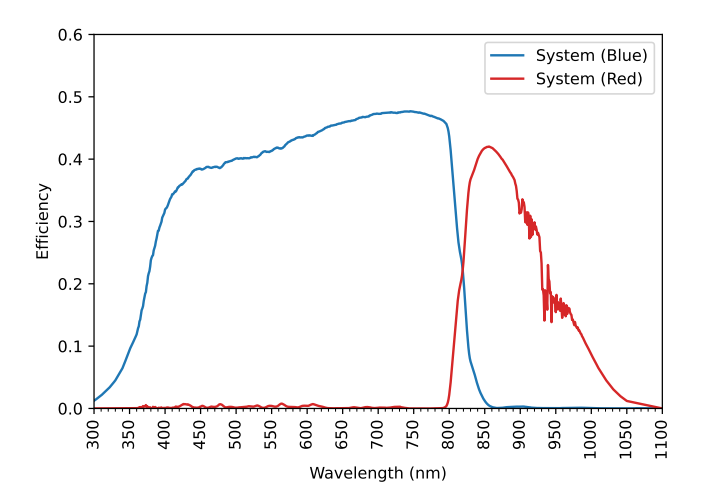
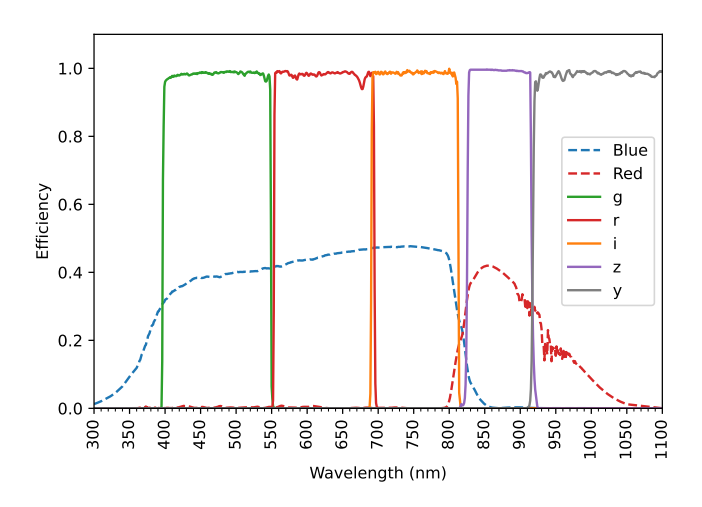


Figure 7.1: Top: The major components of the system efficiency at 1.5 airmasses: the atmosphere, telescope, and the efficiencies of the blue and red channels of the instrument without filters. Bottom: The system efficiencies of the blue and red channels without filters.



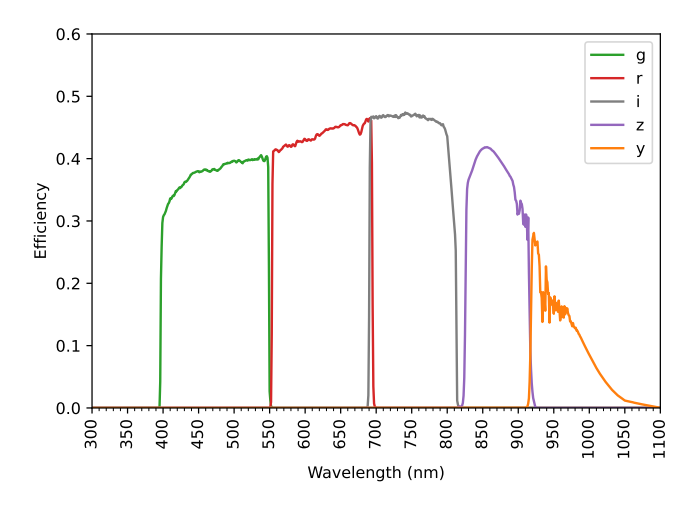
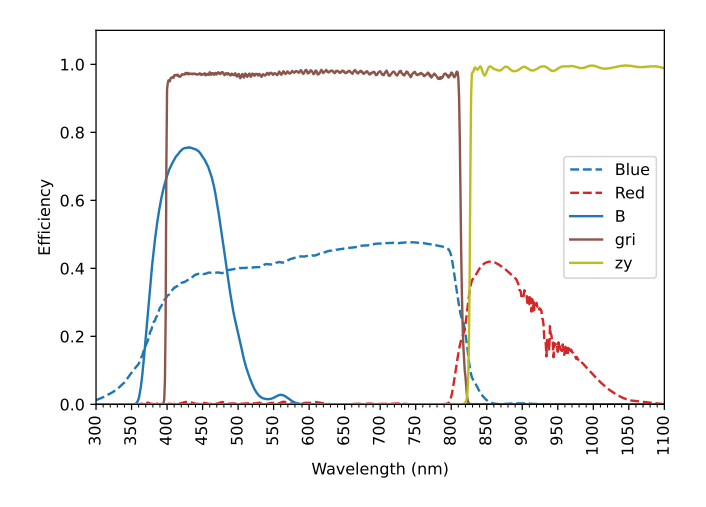


Figure 7.2: Top: the transmission of the g, r, i, z, and y filters and the system efficiencies of the blue and red channels without filters. Bottom: the system efficiencies including the g, r, i, z, and y filters. Note that the D2 dichroic encroaches on the red edge of the i filter and the blue edge of the i filter.



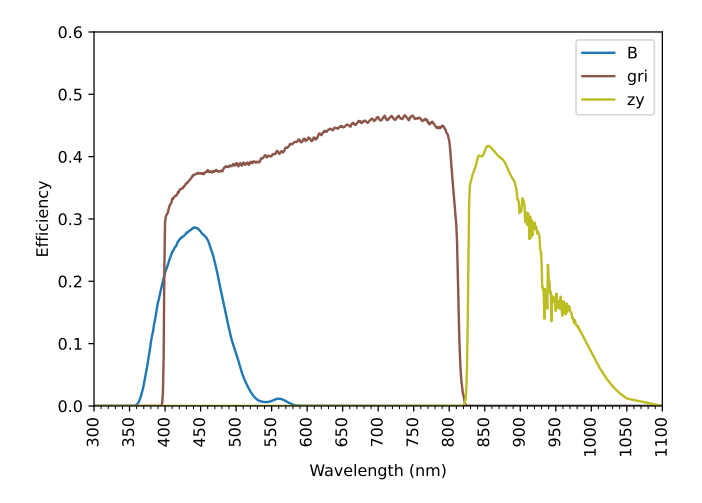
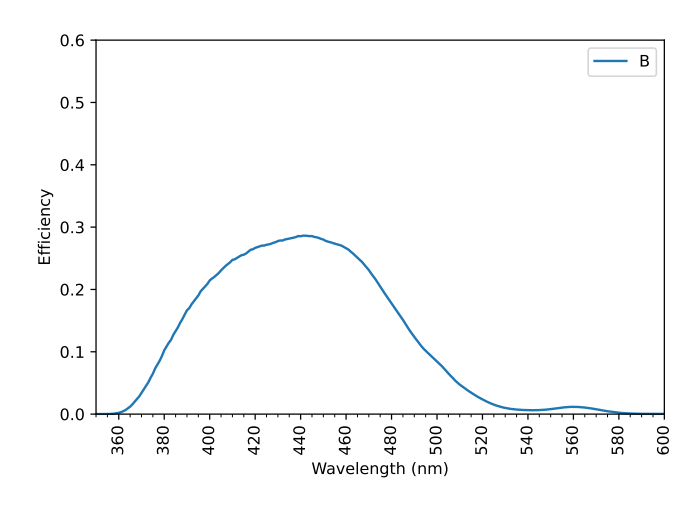


Figure 7.3: Top: the transmission of the B, gri, and zy filters and the system efficiencies of the blue and red channels without filters. Bottom: the system efficiencies including the B, gri, and zy filters. Note that the D2 dichroic encroaches on the red edge of the gri filter and the blue edge of the zy filter.



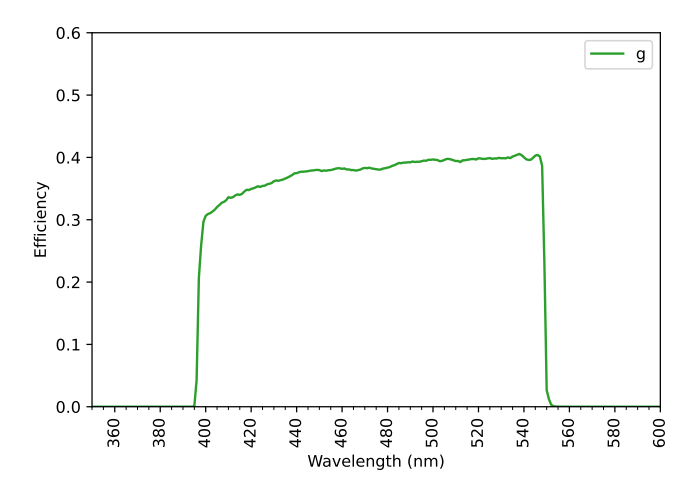
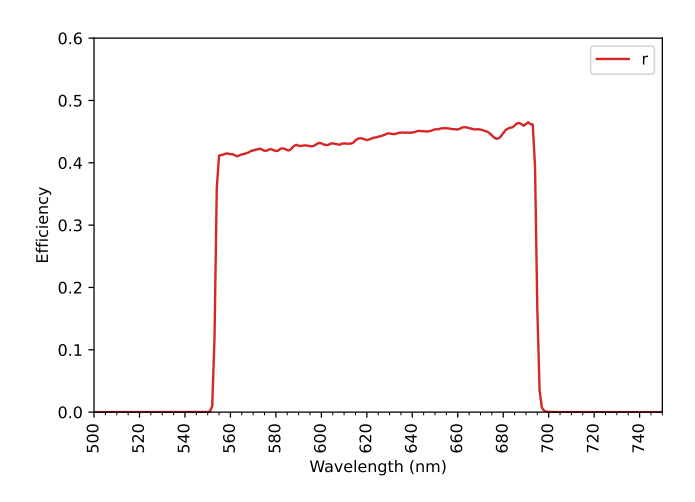


Figure 7.4: The system efficiencies in the B and g filters.



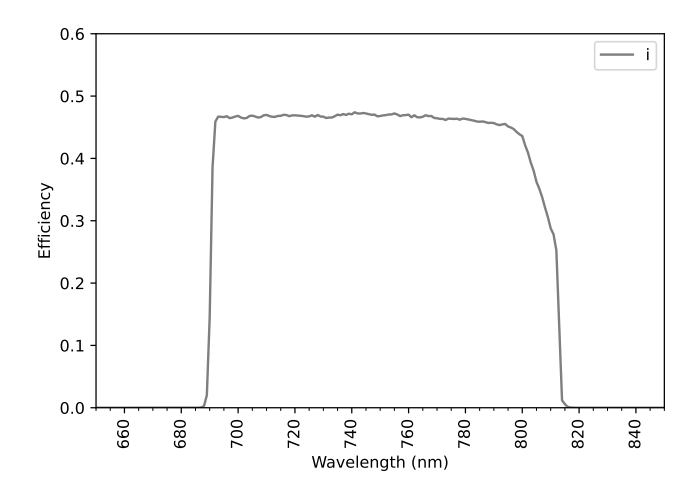
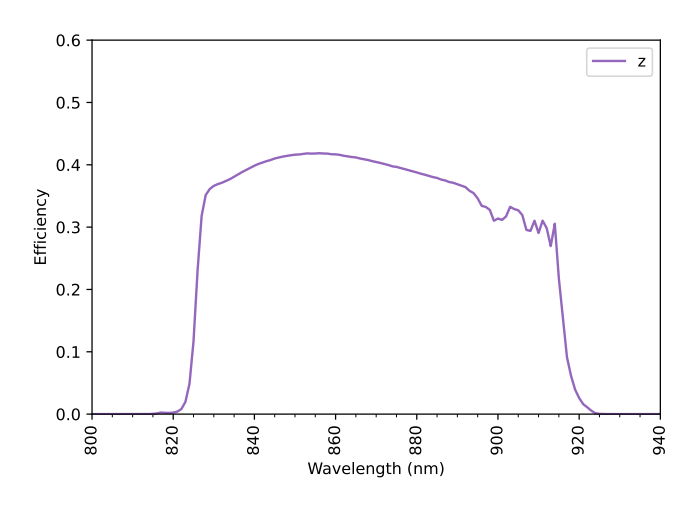


Figure 7.5: The system efficiencies in the r and i filters.



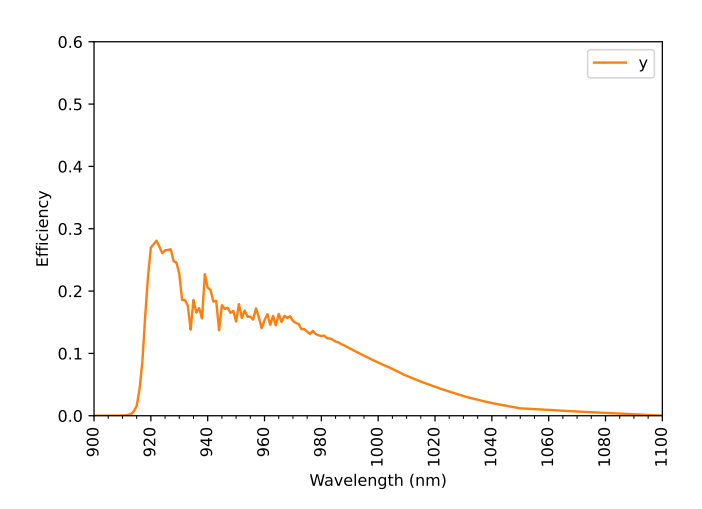
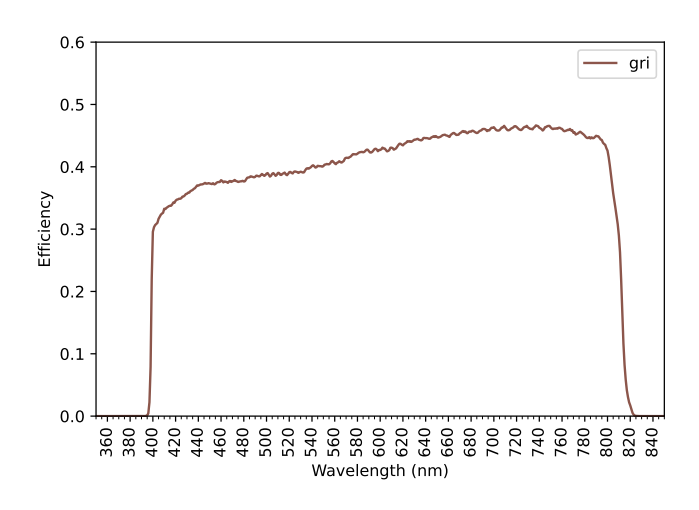


Figure 7.6: The system efficiencies in the z and y filters.



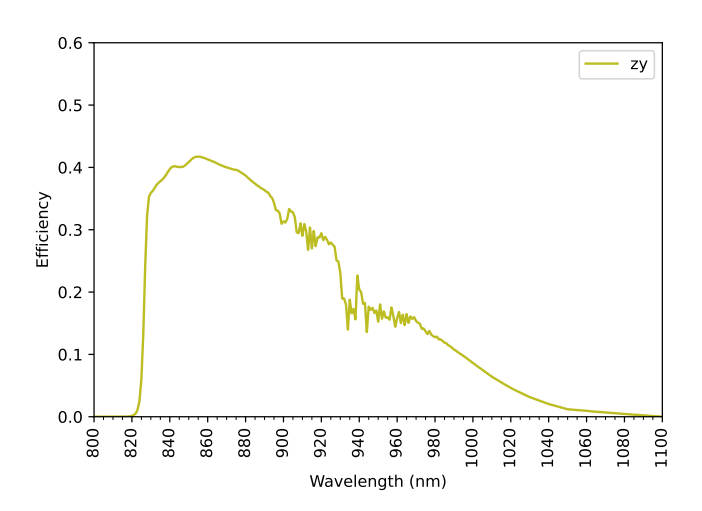


Figure 7.7: The system efficiencies in the gri and zy filters.

Detectors

The instrument uses two Spectral Instruments 1110S CCD detector systems, each with a backside-illuminated e2v 231-84 CCD. These detectors have a format of $4k\times 4k$ with 15 μm pixels. The detectors have the "astro multi-2" AR coating and deep-depleted silicon. The red detector also has e2v's fringing-suppression treatment. They are cooled by a Brookes Polycold® PCC Compact Cooler with PT-30 refrigerant. Each detector has an integrated Vincent/Uniblitz CS90HS1T0 shutter.

8.1 Detectors and Channels

The detectors can be identified by the value of the DTDS record in the FITS header. The value is 'SI 1110-167' for the blue detector and 'SI 1110-185' for the red detector.

The channel can be identified by the value of the INSTRUME record in the FITS header. The value is 'C1' for the blue channel and 'C2' for the red channel.

Note that:

- From 2025-01-05 until 2025-03-10, the blue CCD was installed in the blue channel, but the red CCD was not in service.
- ullet From 2025-03-19 until 2025-08-27, while the blue detector was being repaired, the red detector was installed in the blue channel.
- Since 2025-08-30, both detectors have been installed in their corresponding channels.

8.2 Read Modes

The hardware controller offers read frequencies of 1.01 MHz, 502.5 kHz, and 332.2 kHz, and low- and high gain modes. Combinations of these are exposed by the instrument control system as "read modes".

The only read mode supported for science observations is read mode 0, which combines the 1.01 MHz read frequency and the low amplifier gain of about 2 electrons per DN. This combines fast readout of about 7 seconds, reasonable read noise of 7 electrons, and the deepest full-well of about 140,000 electrons (Watson 2020).

8.3 Format

Both detectors have an active area of 4096 columns \times 4112 rows. The controller reads them using the "split full frame read-out through four amplifiers" scheme (Teledyne e2v 2018, p. 17) with 50 columns of underscan at the start and end of each row, giving a total size of 4196 columns \times 4112 rows divided into four quadrants. This is shown in Figure 8.1. Each quadrant has slightly different bias level and gain, and this gives a clear pattern in raw exposures. However, subtracting the underscan level and residual bias and dividing by a flat field largely removes these differences.

We do not typically use the full native format. In the laboratory, the first and last rows showed unusual behavior, with higher values in the underscan regions and lower values in the active regions (Watson 2020). Also, the underscan regions of 50 columns are not commensurate with a binning of 4. However, the full native format is available as an engineering mode with window name full.

The controller allows us to define windows provided they are centered on the detector. We define three windows that we expect will be useful for science, named 4kx4k, 2kx2k, and 1kx1k, described below and shown in Figure 8.1. Each window can be used with a binning of 1, 2, or 4 pixels (both vertically and horizontally).

• The 4kx4k window has an active area of 4096 columns × 4096 rows,

Table 8.1: Detector Gain and Read Noise

	Blue	Red
Gain (e/DN)	2.2	2.1
Read Noise (e)	6.8	7.0

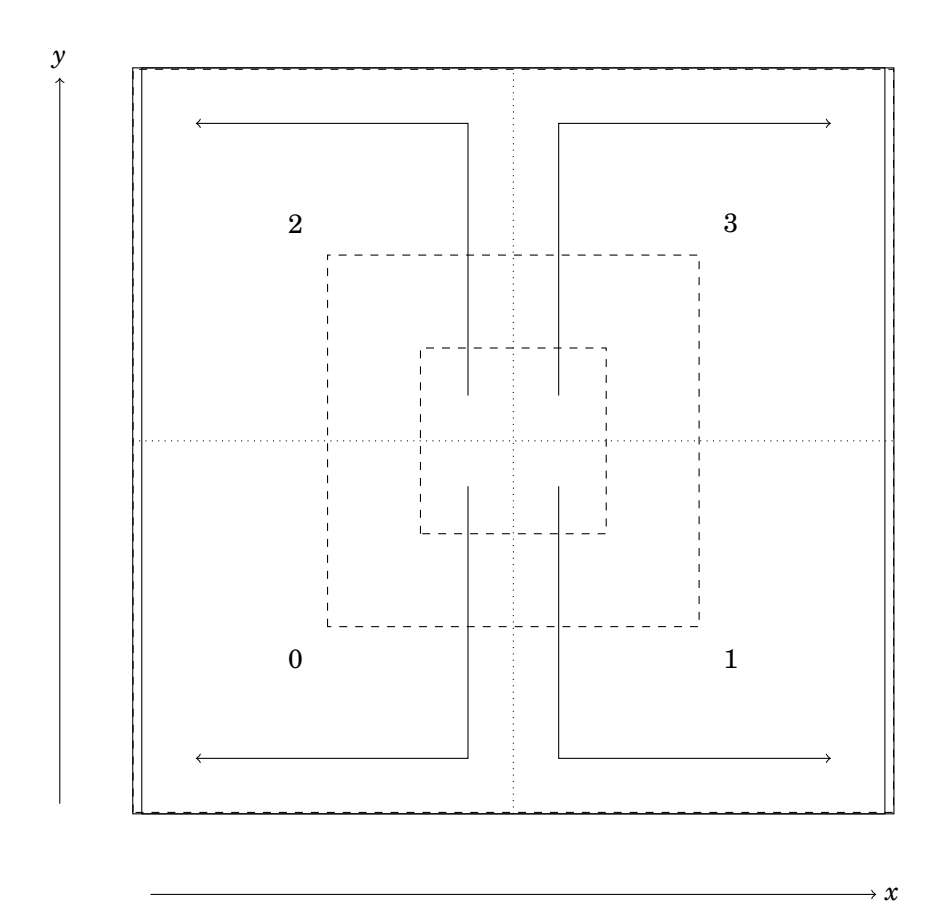


Figure 8.1: The format of the CCD. The full format has an active area of 4096 columns \times 4112 rows and with 50 columns of underscan at the start and end of each row, giving a total format of 4196 columns \times 4112 rows. It is read in four quadrants, as shown by the dotted line and the arrows. The parallel clocks move charge vertically, and the serial clocks move charge horizontally. The quadrants are numbered 0 to 3 as shown. The dashed lines show the 4kx4k, 2kx2k, and 1kx1k windows.

centered on the detector, with 48 columns of underscan at the start and end of each row, giving a total size of 4192 columns × 4096 rows.

- The 2kx2k window has an active area of 2048 columns × 2048 rows, centered on the detector, without underscan.
- The 1kx1k window has an active area of 1024 columns × 1024 rows, centered on the detector, without underscan.

We anticipate that almost all science will use the standard 4kx4k window with a binning of 1. The other windows and binnings are likely to be of interest only for fast (or at least faster) photometry, and their use requires making special arrangements with the science operations team.

Table 8.2 shows the measured overhead times (reset, read, and other overheads associated with each exposure) for each of the windows and binnings. The overhead for the standard 4kx4k window with a binning of 1 is about 7 seconds. The fastest combination is the 4kx4k window with a binning of 4 (i.e., pixels of 1.5 arcsec), which has an overhead of 2.4 seconds.

8.4 Bias and Dark Correction

8.4.1 Bias Pedestal Removal

Table 8.3 shows the slices corresponding to each quadrant, underscan region, and data region. These are given as Python slices; to convert them into IRAF sections, reverse the order and add one to the first index. For other binnings, divide all numbers by the binning.

The procedure for removing the bias pedestal level from 4kx4k images and extracting the data region is:

- Determine the mean value in the underscan slice in each quadrant.
- Subtract these values from the whole quadrant slice.
- Extract either the individual data slices for each quadrant or the combined data slice for all quadrants.

This procedure is carried out automatically by the COLIBRÍ pipeline.

If you wish to carry out this step yourself on raw 4kx4k images with binning 1, the engineering team recommends this code:

```
import astropy.stats
p0 = astropy.stats.sigma_clipped_stats(data[ 0:2048, 0: 48])[0]
p1 = astropy.stats.sigma_clipped_stats(data[ 0:2048,4144:4192])[0]
p2 = astropy.stats.sigma_clipped_stats(data[2048:4096, 0: 48])[0]
p3 = astropy.stats.sigma_clipped_stats(data[2048:4096,4144:4192])[0]
```

```
data[ 0:2048, 0:2096] -= p0
data[ 0:2048,2096:4192] -= p1
data[2048:4096, 0:2096] -= p2
data[2048:4098,2096:4192] -= p3
data = data[0:4096,48:4144]
```

Conventional bias pedestal correction is not possible for images taken with the 2kx2k and 1kx1k windows as they do not include underscan regions.

8.4.2 Residual Bias and Dark Correction

We recommend a slightly non-standard approach to residual bias and dark correction: instead of subtracting a residual bias and a scaled dark image, subtract a dark image of the same exposure time. The reason is that we suspect that the residual bias levels of images taken in rapid succession vary at the level of ± 0.3 DN (Watson 2023). Furthermore, the detectors are operated at -110 C and their median dark current is essentially unmeasurable.

8.5 Orientation on Sky

To simplify cable handling, the telescope derotator is only capable of rotating the DDRAGO instrument through ± 65 degrees. This means that we cannot maintain the same field orientation on the detector at all positions. However, we step the derotator offset in multiples of 90 degrees so that North is always approximately aligned with either the columns or rows. The value of the derotator offset is given in the SMTMRO record in the image header.

If you wish to correct the orientation of raw data yourself, the engineering team recommends this code:

```
if header["INSTRUME"] == "C2":
    data = np.flipud(data)
rotation = header["SMTMRO"]
data = np.rot90(data, -int(rotation / 90))
```

The center of rotation is close to but not precisely coincident with the center of the detector.

Table 8.2: Detector Overhead Times

Window	Binning	Overhead s
4kx4k	1	7.0
4kx4k	2	3.5
4kx4k	4	2.4
2kx2k	1	5.1
2kx2k	2	3.9
2kx2k	4	3.4
1kx1k	1	4.7
1kx1k	2	4.1
1kx1k	4	4.0

Table 8.3: Detector Quadrant, Underscan, and Data Slices

Window	Binning	Quadrant	Quadrant	Underscan	Data
4kx4k	1	0	0:2048, 0:2096	0:2048, 0: 48	0:2048, 48:2096
4kx4k	1	1	0:2048, 2096:4192	0:2048, 4144:4192	0:2048, 2096:4144
4kx4k	1	2	2048:4096, 0:2096	2048:4096, 48:2096	2048:4096, 48:2096
4kx4k	1	3	2048:4096, 2096:4192	2048:4096, 4144:4192	2048:4096, 2096:4144
4kx4k	1	All			0:4096, 48:4144

Bibliography

- Boccas M., Vucina T., Araya C., Vera E., Ahhee C., 2006, TSF, 502, 275. doi:10.1016/j.tsf.2005.07.295
- Fuentes J., Watson A. M., & Cuevas C, 2022, "COLIBRÍ Optical Design," COLIBRI-UNAM-DS-1, Version 8.2
- Langarica R., Watson A. M., Álvarez Núñez L. C., Angeles F., Atteia J.-L., Basa S., Cuevas S., et al., 2024, SPIE, 13096, 130963D. doi:10.1117/12.3020545
- Otárola A., Hiriart D., Pérez-León J. E., 2009, RMxAA, 45, 161
- Schuster W. J., Parrao L., 2001, RMxAA, 37, 187
- Spectral Instruments, 2014, "Series 1100/1110 Camera System Service Cabinet Modular Version Service Manual,"
- Teledyne e2v, 2018, "CCD231-84 Back-illuminated Scientific Sensor," A1A-765136 Version 8
- Tonry J. L., Stubbs C. W., Lykke K. R., Doherty P., Shivvers I. S., Burgett W. S., Chambers K. C., et al., 2012, ApJ, 750, 99. doi:10.1088/0004-637X/750/2/99
- Watson A. M., 2020, "DDRAGUITO: Detector and Filter Wheel Laboratory Verification," Version 1.0.
- Watson A. M., 2023, "DDRAGUITO: Analysis of Commissioning Data," Version 1.1.
- Watson A. M., 2018, "COLIBRI Expected Performance," Alan Watson, GFT-AN-A3135-046-UNAM, Version 2.1